

10-1-1998

Layer-thickness dependence of the conductive properties of Mo/Si multilayers

Gregory S. Elliott

University of Puget Sound, gelliott@pugetsound.edu

Adam D. Gromko

University of Puget Sound

Francis VandeVeegaete

University of Puget Sound

Christopher D. Johnson

Department of Chemistry, University of Oregon, Eugene, Oregon 97403

David C. Johnson

Department of Chemistry, University of Oregon, Eugene, Oregon 97403

Follow this and additional works at: http://soundideas.pugetsound.edu/faculty_pubs

Citation

Elliott, Gregory S., Ad Gromko, Fv Veegaete, Cd Johnson, et al. 1998. "Layer-thickness dependence of the conductive properties of Mo/Si multilayers." *Physical Review B* 58(13): 8805-8811.

This Article is brought to you for free and open access by the Faculty Scholarship at Sound Ideas. It has been accepted for inclusion in All Faculty Scholarship by an authorized administrator of Sound Ideas. For more information, please contact soundideas@pugetsound.edu.

Layer-thickness dependence of the conductive properties of Mo/Si multilayers

Greg S. Elliott, Adam D. Gromko, and Francis VandeVeegaete
Department of Physics, University of Puget Sound, Tacoma, Washington 98416

Christopher D. Johnson and David C. Johnson
Department of Chemistry, University of Oregon, Eugene, Oregon 97403
(Received 19 March 1998)

We report new measurements of the conductance and superconducting transition temperature of a set of Mo/Si multilayers, as a function of the metal layer thickness (from 7–85 Å) for a constant semiconductor layer thickness of 22 Å. Unlike previously reported measurements, we do not observe oscillations in either the resistivity, resistivity ratio, or the superconducting transition temperature with the metal layer thickness. Rather, we observe monotonic variations in the transport properties as the metal layer thickness increases. The sheet conductance and its change between 10 and 300 K both vary approximately linearly with the metal layer thickness, above a threshold thickness. The conductance starts to grow with metal layer thickness at approximately 10 Å, whereas the temperature coefficient of resistance changes sign at approximately 25 Å, exhibiting a Mooij correlation with a crossover resistivity of 125 $\mu\Omega$ cm. The observed temperature dependence of the conductance rules out localization as the origin of the negative temperature coefficient of resistance. The conductance data are analyzed using a simple phenomenological model involving transport in interfacial and metallic layers, whose relative contribution to the conductance depends on the metal layer thickness and the temperature. The model is applied to separate two competing contributions that determine the overall temperature dependence of the conductance. We attribute the differences between our measurements and previous measurements to differences in bulk metallic conductivities and interface morphologies, due to differences in thermal evaporation versus sputtering fabrication processes. Our results show that the level and nature of disorder is an important ingredient in any theory that explains the cause of the observed oscillations.

[S0163-1829(98)04337-9]

I. INTRODUCTION

A previous set of measurements of electrical conduction in Mo/Si multilayers report oscillations in the metal layer thickness dependence of the resistivity, the residual resistance ratio, the superconducting critical temperature, and the temperature derivative of the transverse critical field.^{1,2} Initially, this observation was associated with a quantum size effect, although the normal conditions for such an effect are not met in these films. Analysis of the temperature dependence of the resistance and magnetoresistance of several of these Mo/Si multilayers attributes an observed negative temperature coefficient of resistance (TCR) and approach to the superconducting state to quantum interference effects due to weak localization, electron-electron interactions, and superconducting fluctuations.³ An examination of the superconducting transition temperatures for these same films showed that an enhancement of T_c was caused by changes in the electronic structure resulting from disorder, accompanied by a competing effect to reduce T_c that was caused by a rise in sheet resistance for thinner Mo layers.⁴ Another experiment observed no layer thickness oscillations in single layer Mo films, ruling out space quantization as the reason for the size oscillations.⁵ Most recently, oscillations in the anisotropy ratio have been observed in this same set of Mo/Si films, correlating with the other previously reported oscillations.⁶ This experiment indicates that the interlayer coupling strength varies with metal layer thickness, for constant silicon layer thickness.

The intriguing observation of oscillatory transport behavior with metal layer thickness led us to pursue our own investigation of the layer thickness dependence of the conductive properties in this system. We fabricated a set of Mo/Si multilayers over a range of metal layer thicknesses from 7–85 Å, for a constant silicon layer thickness of 22 Å (samples in the previous studies have a molybdenum thickness range from 8–200 Å and a silicon thickness of 25 Å). For each sample, we measured the sheet conductance versus temperature and determined the superconducting transition temperature (if any). We observe similar but distinctly different transport properties than observed in the other studies of this system. We do not observe oscillations in either the resistivity, resistivity ratio, or the superconducting transition temperature with the metal layer thickness. The main differences between the two sample sets is in the magnitude of the conductivity, and in the nature of the scattering processes that determine the conductivity. Our results imply that the level and nature of the disorder are important factors in the cause of the observed oscillations. In what follows, we describe our sample preparation and experimental techniques, present and discuss our results, make comparisons with results from the other studies of this system, and present a simple conduction model that explains the observed layer thickness and temperature dependences.

II. SAMPLE PREPARATION AND CHARACTERIZATION

The Mo/Si multilayers used in this study were made in an ultrahigh vacuum deposition system which has been de-

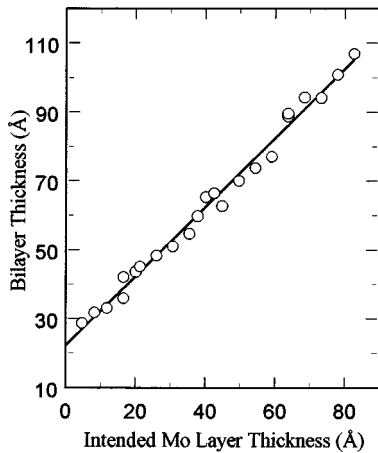


FIG. 1. Bilayer thickness, as measured by x-ray diffraction, is plotted versus the intended molybdenum layer thickness, as measured by the crystal thickness monitor during deposition. The bilayer thickness was calculated as an average over the higher order diffraction peaks, only using peaks above 2.5° to avoid refractive corrections. A linear best fit to the data yields an intercept of $22 \pm 1 \text{ \AA}$. This value for the average silicon layer thickness was used to calculate a molybdenum layer thickness for each sample.

scribed in detail elsewhere.⁷ Briefly, both elements were deposited in succession on optical quality glass substrates at a rate of 0.5 \AA/s , using electron-beam heated sources controlled by quartz crystal monitors. In the main set of samples described in this paper, the intended silicon layer thickness was held constant at approximately 20 \AA , and the intended molybdenum layer thickness was varied from about 7 \AA up to 85 \AA , in steps of $3\text{--}4 \text{ \AA}$. Four copies of each multilayer were made simultaneously, and all multilayers in this study consist of twenty molybdenum-silicon bilayers, with molybdenum deposited last. Low angle x-ray diffraction from the multilayers was performed to determine the average bilayer period; diffraction was typically observable out to 8° , or up to sixth order for samples with thicker molybdenum layers. High angle diffraction measurements indicate the presence of crystalline molybdenum for films with metal layers thicker than about 20 \AA , with a crystallite size perpendicular to the layers that scales with the layer thickness up to 100 \AA (the thickest layers investigated). Further work on powdered samples is needed to determine if the crystallite size is the same in the plane of the layers. Figure 1 shows a graph of the bilayer spacing, as measured by x-ray diffraction, plotted versus the intended molybdenum layer thickness, as measured during deposition by the crystal thickness monitor, for a set of 23 Mo/Si multilayers films. The bilayer spacing was calculated as an average over the higher-order diffraction peaks; peaks below 2.5° were not included to avoid making a refractive correction. A linear best fit to this data yields an intercept of $22 \pm 1 \text{ \AA}$, corresponding to an average silicon layer thickness. A molybdenum layer thickness for each sample is calculated as the difference of the actual bilayer thickness and this average silicon layer thickness.

Electrical conductivity measurements were made on each sample using the van der Pauw technique.⁸ The samples were fabricated in the shape of a plus sign, or cross, with rounded inside corners. The width of the arms of the cross is 0.75 mm , and the diameter of the cross is 1 cm . Four 0.1

mm-diam. copper electrical leads were attached to the four ends of the cross using silver paint. I - V measurements were made over a range of currents, typically from 0.1 to 1.0 mA , in the eight van der Pauw resistivity configurations. The redundancy of these measurements has several advantages: (1) it permits a determination of the sheet resistance without geometric scaling, (2) two values for the sheet resistance are determined by the measurement, providing a reliability check, and (3) changes in the distribution of current in the sample can be monitored. A disadvantage is that the current flow is two dimensional, which unlike one dimensional flow in a long, narrow sample can be altered by changes in the injection of current into the sample at the contacts. However, advantage (3) does allow one to determine if this is occurring during the measurement process. The cross shape minimizes this problem because the current distribution in the center of the cross, which determines the measured voltages, is relatively insensitive to changes in the distribution of injected current at the ends of the cross arms.⁹

Van der Pauw I - V curves were measured for each sample as a function of temperature, using two different cryostats. A closed-cycle helium refrigerator was used in the temperature range from 10 K up to room temperature, and a flow through helium cryostat was used from 1.8 up to 15 K . In the lower temperature range, the temperature was varied linearly in time at 0.5 K/min , and the conductance data was taken continuously, with one conductance data point taking 5 s to acquire. This rate was slow enough that no hysteresis was observed in the superconducting transition measurement. Except in a few samples, the transition region was wider than the temperature resolution set by this finite rate. In the higher temperature range, the sample temperature was varied at 1 K/min . Above the superconducting transition, all the I - V curves showed ohmic behavior.

III. EXPERIMENTAL RESULTS AND DISCUSSION

The room-temperature sheet conductances for the 23 Mo/Si multilayers are plotted versus molybdenum layer thickness in Fig. 2. As one might expect, there is an increase in the conductance with increasing metal layer thickness. Also apparent is a fair amount of scatter in the data. The uncertainty in the measured value of the conductance is typically less than 1% , and successive measurements yield the same values over a period of months. The uncertainty in the molybdenum layer thickness is on the order of a few angstroms. Neither of these uncertainties can account for the apparent scatter. In a series of ten “identical” samples, made simultaneously in the same deposition sequence, the measured conductances varied over a 10% range. Thus the scatter is not correlated to the molybdenum layer thickness (as measured by x-ray diffraction), and appears to be intrinsic to the fabrication process. This variation must be associated with differences in other contributions to the resistivity, most likely in the nature of the interfaces or in other forms of disorder.

The general linear trend of the room-temperature data in Fig. 2 does not appear to cross the origin, implying that a minimum amount of metal is needed before appreciable conduction can occur. Beyond this minimum amount, the increase of the sheet conductance with the additional metal

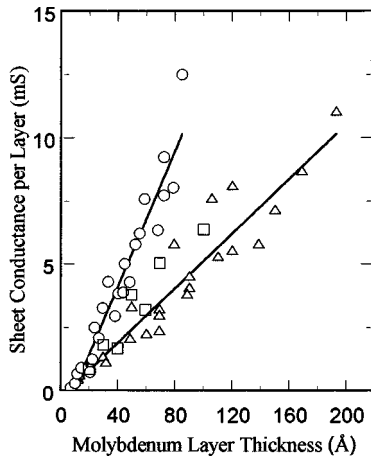


FIG. 2. Room-temperature sheet conductance is plotted versus molybdenum layer thickness. Circles (\circ) are for Mo/Si multilayers from this work. Triangles (\triangle) and squares (\square) are a close approximation to the data of Fogel *et al.* for Mo/Si multilayers and for single Mo films, digitized from Fig. 1 of Ref. 4, and inverted to plot conductance vs layer thickness. The best linear fit to the two Mo/Si data sets are shown, with the slopes yielding resistivities of $75 \mu\Omega \text{ cm}$ and $185 \mu\Omega \text{ cm}$.

layer thickness also suggests that the conduction is primarily occurring in the metal layers. Calculating the resistivity as the inverse of the slope of the line joining the origin and the data points in Fig. 2, we find that the resistivity decreases from about $400 \mu\Omega \text{ cm}$ to $100 \mu\Omega \text{ cm}$ as the metal layer thickness increases from 7 \AA to above 40 \AA . Alternatively, a linear model allowing for a nonzero intercept yields a best-fit slope corresponding to a resistivity of $75 \pm 4 \mu\Omega \text{ cm}$, and a best fit for the horizontal intercept of $10 \pm 4 \text{ \AA}$. Also shown in Fig. 2 is an approximation to the data of Fogel *et al.*, for Mo/Si multilayers as well as for single Mo films sandwiched between Si layers. This data was digitized from Fig. 1 of Ref. 4, and inverted to plot conductance versus molybdenum layer thickness (rather than resistance versus inverse layer thickness). Plotting the data in this manner allows one to visually inspect the behavior of the conductivity at small metal thickness as an approach to the origin, rather than a divergence of R at large values of inverse metal thickness. Clearly, the two multilayer samples sets have different metallic conductivities, and hence different levels of disorder in the metallic component. A fit to the data of Fogel *et al.* in this form yields a resistivity of $185 \pm 10 \mu\Omega \text{ cm}$, and a horizontal intercept of $5 \pm 6 \text{ \AA}$.¹⁰ An offset in the horizontal intercept is not as apparent in their data set; this may be due to a more graded compositional profile for sputtered samples, as we discuss below.

The temperature dependence of the sheet conductance of several multilayers spanning a range of molybdenum layer thickness are plotted in Fig. 3, normalized to their value at 290 K. The temperature dependence for all multilayers with molybdenum layers thicker than about 25 \AA are qualitatively similar; for clarity, only one of these curves is shown, for $d_{\text{Mo}} = 30 \text{ \AA}$. The films with molybdenum layers thicker than 25 \AA all exhibit a small percentage drop in conductance from 10 to 290 K, with a superconducting transition observed at low temperatures ($2\text{--}6 \text{ K}$). These conductance versus temperature curves are all practically linear, with a negative

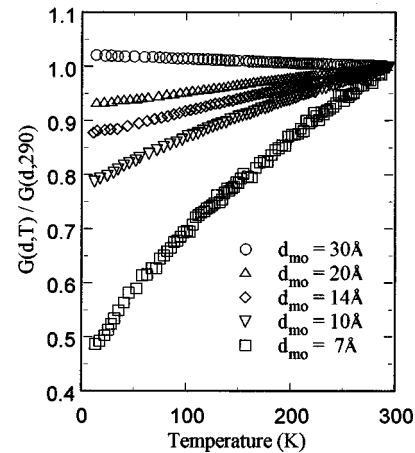


FIG. 3. Normalized sheet conductance $G(T)/G(290)$ is plotted vs temperature for five samples over a range of molybdenum layer thickness from 7 to 30 \AA . All samples with a molybdenum layer thickness d_{Mo} less than about 25 \AA exhibit a negative temperature coefficient; all samples with d_{Mo} above 25 \AA exhibit a positive temperature coefficient.

slope (corresponding to a positive TCR). For multilayers with molybdenum layer thicknesses less than about 25 \AA , the sheet conductance increases with increasing temperature, and the conductance versus temperature curves have a positive slope (a negative TCR), and show a slight negative curvature. The slope and curvature both increase with decreasing metal layer thickness. This effect grows to be very large; for the film with the thinnest metal layers (7 \AA), the conductance changes over 200% from 10 to 290 K. Also, the superconducting transition drops below 1.8 K (our lower temperature limit) as the layer spacing decreases, and perhaps is suppressed altogether.

There appears to be two competing effects that determine the temperature dependence of the conductance. Both effects are monotonic in temperature, one having a positive, constant temperature derivative and the other a negative, varying one. The contribution of each effect to the overall temperature dependence depends on the metal layer thickness, and the two effects balance each other at a layer thickness of 25 \AA . The small but positive TCR is characteristic of conduction in a disordered metal, with defect scattering dominating inelastic scattering. A negative TCR can result from a variety of different processes in disordered metals, for example, weak localization or a temperature dependent elastic scattering process. This interplay between two competing contributions to the TCR was first observed by Mooij,¹¹ who found a correlation between the sign and magnitude of the TCR with the resistivity, with a zero TCR occurring at a crossover resistivity of about $100\text{--}150 \mu\Omega \text{ cm}$. Many systems show a similar correlation, but over a wider range of crossover resistivities.¹² A Mooij correlation graph for our sample set is shown in Fig. 4. The TCR for each sample was calculated at room temperature, and the resistivity was calculated using the metal layer thickness determined by x-ray diffraction. Our samples have a crossover resistivity in the neighborhood of $125 \mu\Omega \text{ cm}$. This low value of the crossover resistivity rules out weak localization as the origin of the negative TCR effect.^{12,13} At low resistivities, weak localization predicts a negative TCR only at low temperatures. Except in the region

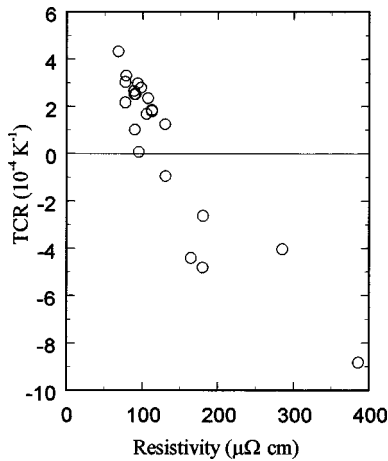


FIG. 4. A Mooij correlation plot showing the temperature coefficient of resistance (TCR) versus the resistivity for all the samples in this study. The TCR was calculated at room temperature, and the resistivities were calculated using the molybdenum layer thickness determined by x-ray diffraction. A zero TCR occurs at a crossover resistivity of approximately $125 \mu\Omega \text{ cm}$.

of the superconducting transition (all below 10 K), we do not observe a change in the sign of the TCR for *any* sample. Also, the form of the data does not show a $\ln(T)$ or $T^{1/2}$ dependence as predicted for weak localization in two and three dimensions.¹⁴ Another plausible origin of the negative TCR might be a hopping mechanism for a thin, discontinuous layer, however, at a thickness of 25 \AA we would expect the metal layers to be continuous. A log-log plot of the change in conductance from its extrapolated zero-temperature value does not show any single power-law dependence, providing no further evidence for any single mechanism. Other possible mechanisms that could cause a negative TCR could be a semiconducting interfacial layer, charge trapping at the interfaces, or temperature-dependent elastic scattering process, in which the mean-free path increases with increasing temperature. In the absence of experimental evidence differentiating between these possible mechanisms, we simply assume some mechanism is responsible, and in the following section we analyze the $G(d, T)$ conductance data set to deduce parameters describing the temperature dependence of the conductivity of this component.

A condensed version of the temperature dependence of the conductance can be represented for the whole set of multilayers in a plot of the resistance ratio versus layer thickness, shown in Fig. 5. The resistance ratio for our samples was calculated between 290 and 10 K. In the normalized plots of $G(d, T)/G(d, 290)$ versus T in Fig. 3, the resistance ratio can be seen as the values on the curves at the lowest temperature. A negative TCR corresponds to a resistance ratio value between zero and one; a positive TCR corresponds to a resistance ratio value greater than one. Our data clearly shows a single change in the TCR from negative to positive at a layer thickness of about 25 \AA . In the range from 7 to 25 \AA , the resistance ratio increases from about one half up to one. For thicker metal layers, the resistance ratio stays above one and shows a slight increase with layer spacing. The solid line corresponds to a fit to the entire data set, based on a simple, two layer conduction model discussed in the following sec-

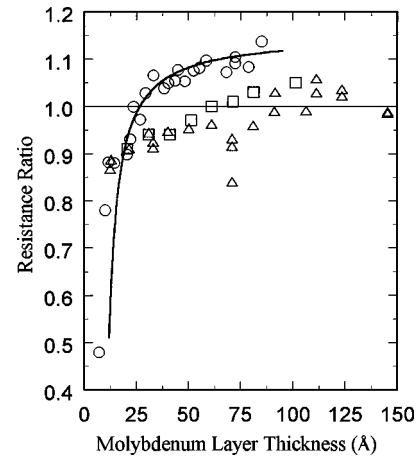


FIG. 5. Resistance ratio is plotted vs molybdenum layer thickness. Circles (\circ) are for Mo/Si multilayers from this study, and are calculated as the ratio of the resistances at 290 K and 10 K. Triangles (Δ) and squares (\square) are a close approximation to the data of Fogel *et al.* for Mo/Si multilayers and for single Mo films, digitized from Fig. 2 of Ref. 5, and are the ratio of the resistances at 290 K and the peak of the $R(T)$ curve. The solid curve is a fit to our data based on the two layer model discussed in the text.

tion. Also shown for comparison in Fig. 2 is an approximation to the resistance ratio data of Fogel *et al.*, for both Mo/Si multilayers and for single Mo films sandwiched between Si layers. This data was digitized from Fig. 2 in Ref. 5. Their resistance ratio is calculated between room temperature and the temperature corresponding to the maximum resistance before the superconducting transition. For this set of multilayers, negative TCR's are observed all the way out to a layer thickness of 200 \AA , and for the single Mo films, the prominent feature observed near 70 \AA in the multilayers is absent.

We also measured the superconducting transition temperature of our films, using the lower temperature cryostat. All samples which superconducted exhibited a sharp transition, but for some of the samples, the sharp transition occurred with a shoulder on either the top, bottom, or both ends of the transition. Perhaps this results from a distribution of layer thickness, or varying levels of disorder. The 10% to 90% width to the transition ranged between 0.1 K up to 3 K due to the shoulders on the transitions. The temperatures at which the sharp transition occurred in the set of 23 multilayers are shown plotted versus molybdenum layer thickness in Fig. 6. A general increasing trend of this transition temperature with layer spacing is apparent, however, there are a few degrees K of scatter to the data. Even with this level of scatter, it does not appear that our samples show an oscillatory dependence of T_c on the metal layer thickness. For films with thinner metal layers, the transition temperature rises from around 2 K up 4–5 K; films with thicker metal layers have transition temperatures in the range from 4 to 5.5 K. For comparison, an approximation to the transition temperature data of Fogel *et al.* is also presented, digitized from Fig. 1 in Ref. 5. The lower T_c range for our data is also consistent with the greater sheet conductivity of our samples.⁴

While we observe the same general trends, there are prominent differences between our data set and that of the other studies. We do not observe oscillations in the resistiv-

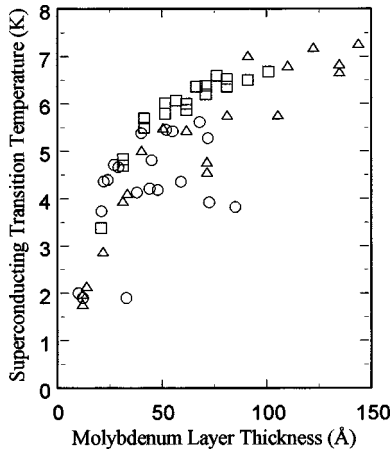


FIG. 6. Superconducting transition temperature is plotted vs molybdenum layer thickness. Circles (○) are for Mo/Si multilayers from this study, triangles (△) and squares (□) are a close approximation to the data of Fogel *et al.* for Mo/Si multilayers and single Mo films, digitized from Fig. 1 of Ref. 5.

ity, the residual resistance ratio, or the superconducting transition temperature with layer thickness. Any oscillatory size effect must therefore depend on some other fundamental difference between the two sets of samples. One obvious difference is in the magnitude of the conductivity, which is different by about a factor of 2 to 3. These different conductivities most likely are a result of the two types of fabrication processes. Studies of the compositional depth profile of thermally evaporated and sputtered samples have been done for the Mo/Si system.^{15,16} For sputtered samples, the interfacial width depends on the order of deposition, with Si on Mo yielding an abrupt interface, but with Mo on Si yielding a broad interface, approximately 25 Å thick. Thermal evaporation sources yielded abrupt interfaces, independent of the order of deposition. Two TEM studies^{17,18} of Mo-Si interfaces on sputtered samples both conclude that the interfaces are 17 Å thick when Mo is deposited on Si, and 10 Å thick when Si is deposited on Mo. The lower conductivity in the sputtered samples may therefore result from scattering from substitutional impurities (silicon in molybdenum) as well as perhaps a greater degree of configurational disorder. The conductivity of sputtered multilayered samples and single layer “sandwiches” (molybdenum between silicon layers) is similar.⁵ This is consistent, since these samples should have similar interfacial and bulk compositional profiles.

Not only is the magnitude of the conductivity different between the two data sets, the nature of the scattering processes responsible for the conductivity are different. For our samples, negative TCR’s are observed only for metal layers thinner than 25 Å, and for these samples weak localization can be ruled out as the dominant scattering mechanism. For samples with metal layers thicker than 25 Å, the observed positive TCR can be explained with ordinary Boltzmann transport processes. For the sample set of Fogel *et al.*, quantum interference effects play an important part in determining the conductivity.³ So while our data does not confirm the presence of the size oscillations, it does imply that the physics underlying the oscillations depends on the presence of strong disorder. Any theory that satisfactorily explains the size oscillations should include disorder, and perhaps weak

localization, as a necessary ingredient. This is the main conclusion of our experiment.

IV. MODEL RESULTS

Independent of the question of size oscillations, our data set can be analyzed to explain the overall trends in the layer thickness dependence of the conductance. The conductivity of the films initially increases with increasing layer thickness, and then levels off. This suggests that the first several angstroms of deposited metal have different conduction properties than the metal deposited subsequently. The data also suggests that the sheet conductance $G(d, T)$ is determined mainly by two effects, which depend on temperature in opposite ways. It is natural to associate these two effects with two regions in the metal layer, an interfacial region and a bulk metal region. The contribution of each effect depends on the overall metal layer thickness d (determined by x-ray diffraction), so to separate them we must first write the extrinsic quantity $G(d, T)$ in terms of intrinsic quantities, and scale out the thickness dependence. For films with metal layers greater than some minimum thickness d_{\min} , we assume that the interfacial regions are fully formed and have the same thickness. For these films, we assume that the sheet conductance increases linearly with molybdenum layer thickness, and write

$$G(d, T) = \alpha(T)d + \beta(T), \quad d > d_{\min}, \quad (1)$$

where $\alpha(T)$ and $\beta(T)$ are intrinsic functions to be determined from the data set. In the neighborhood of d_{\min} , $G(d, T)$ must have some different functional form to describe a partially formed interface. Our data set does not warrant an attempt to describe the physics in this region, so we attempt only to model the conductance in films where the above model is plausible. Although there is scatter in the absolute conductance versus molybdenum layer thickness at constant temperature (Fig. 2), relative changes in the conductance with temperature are much more consistent, as evidenced in Fig. 5. Thus we have reason to believe that the functions $\alpha(T)$ and $\beta(T)$ will describe the appropriate trends with temperature in the data set. Examining Fig. 3, since the conductance G is nearly linear in T for films with a positive TCR, and only slightly curved for films with a negative TCR, we expect the functions $\alpha(T)$ and $\beta(T)$ to also be approximately linear in T . Applying a linear least squares fit of the above model to the data set at a sequence of temperatures, we have extracted the functions $\alpha(T)$ and $\beta(T)$. Table I shows the values of these functions and their derivatives extrapolated to $T=0$ K. The function α has a positive slope, whereas β has a negative slope. Graphs of the model fit using Eq. (1) are shown with the experimental data in Figs. 2 and 5. The agreement is adequate in Fig. 2, and good in Fig. 5, indicating that the separable form in Eq. (1) is reasonable.

With further assumptions the functions $\alpha(T)$ and $\beta(T)$ can be expressed in terms of physical quantities. We write the total sheet conductance as the sum of the conductances G_i and G_m of distinct interfacial and metallic layers,

$$G(d, T) = G_i(d, T) + G_m(d, T). \quad (2)$$

TABLE I. Some best fit values for parameters of the two layer conduction model are tabulated; see the text for details.

Model parameter	Best fit value
d_i	11 Å
$\alpha(0)$	3.0×10^5 S/cm
$d\alpha/dT$	-1.3×10^2 S/cm/K
$\beta(0)$	-3.3×10^{-2} S
$d\beta/dT$	3.0×10^{-5} S/K
$\sigma_m(300)$	1.3×10^4 S/cm
$d\sigma_m/dT$	-6.5 S/cm/K
$\sigma_i(300)$	2.1×10^3 S/cm
$d\sigma_i/dT$	7.1 S/cm/K

This model replaces a graded conductivity profile with two adjacent homogeneous layers; we assume that the deduced conductivity of these artificial layers will represent some appropriate average of the true physical situation. The metal layer contribution to the conductance can be written in terms of the number of layers N , the average conductivity per layer σ_m , and the thickness of the layers $d - d_i$,

$$G_m(d, T) = N\sigma_m(T)(d - d_i), \quad (3)$$

where d is the thickness of the molybdenum layer determined by x-ray diffraction, and d_i is the thickness of the interfacial layer. Similarly, the contribution of the interfacial layers to the conductance can be written in terms of an interfacial conductivity σ_i ,

$$G_i(d, T) = N\sigma_i(T)d_i. \quad (4)$$

This physical model is also linear, and the quantities d_i , $\sigma_i(T)$, and $\sigma_m(T)$ can be written in terms of $\alpha(T)$ and $\beta(T)$. We determine the interfacial thickness d_i by the additional condition that $\sigma_i(0) = 0$, and find that

$$d_i = -\beta(0)/\alpha(0), \quad (5)$$

$$\sigma_m(T) = \alpha(T)/N, \quad (6)$$

$$\sigma_i(T) = [\beta(0)\alpha(T) - \alpha(0)\beta(T)]/[N\beta(0)]. \quad (7)$$

Determined in this way, d_i is an effective interfacial width that separates the total molybdenum layer thickness d in a particular fashion. The interfacial part of width d_i has a negative TCR, with a conductance that vanishes at 0 K, much like a semiconductor. The remaining part has a width $(d - d_i)$, and a positive TCR, like a metal. The interfacial thickness parameter d_i is calculated to be 11 Å; essentially this is the horizontal intercept of a plot like Fig. 2 extrapolated to zero temperature. This narrow width is consistent with the abrupt interfaces observed in the compositional depth profile study.¹⁶ Table I also lists some values of the functions $\sigma_i(T)$ and $\sigma_m(T)$ and their derivatives. The room-temperature conductivities of the interfacial and metallic regions differ by almost an order of magnitude, whereas their temperature derivatives are nearly the same, but of opposite sign. The corresponding room temperature resistivities of the two regions are $\rho_i = 480 \mu\Omega \text{ cm}$ and $\rho_m = 77 \mu\Omega \text{ cm}$, in agreement with the observation that the overall resistivity varies from about 400 to 100 $\mu\Omega \text{ cm}$ as the metal layer thickness varies from 7 Å to above 40 Å. The model also predicts a metal layer thickness d_c at the crossover resistivity, where the sheet conductance is independent of temperature,

$$d_c = -\beta'(T)/\alpha'(T) = (1 - \sigma_i'/\sigma_m')d_i \cong 2d_i, \quad (8)$$

which is in good agreement with the observed thickness at the crossover resistivity of 25 Å.

ACKNOWLEDGMENTS

Acknowledgment is made to the donors of the Petroleum Research Fund, administered by the ACS, for partial support of this research. This work was also supported by NSF Grant No. DMR-9510562 at the University of Oregon and NSF Grant No. DUE-9552279 at the University of Puget Sound. Additional support was provided by the Murdock Charitable Trust.

¹V. Y. Kashirin, N. Y. Fogel, V. G. Cherkasova, E. I. Buchstab, and S. A. Yulin, *Physica B* **194–196**, 2381 (1994).

²E. I. Bukhshtab, V. Y. Kashirin, N. Y. Fogel, V. G. Cherkasova, V. V. Kondratenko, A. I. Fedorenko, and S. A. Yulin, *Fiz. Nizk. Temp.* **19**, 704 (1993) [*Low Temp. Phys.* **19**, 506 (1993)].

³E. I. Buchstab, A. V. Butenko, N. Ya. Fogel, V. G. Cherkasova, and R. L. Rosenbaum, *Phys. Rev. B* **50**, 10 063 (1994).

⁴N. Ya. Fogel, E. I. Buchstab, A. S. Pokhila, A. I. Erenburg, and V. Langer, *Phys. Rev. B* **53**, 71 (1996).

⁵N. Ya. Fogel, O. A. Koretskaya, A. S. Pokhila, V. G. Cherkasova, E. I. Buchstab, and S. A. Yulin, *Fiz. Nizk. Temp.* **22**, 359 (1996) [*Low Temp. Phys.* **22**, 277 (1996)].

⁶N. Y. Fogel, O. G. Turutanov, A. S. Sidorenko, and E. I. Buchstab, *Phys. Rev. B* **56**, 2372 (1997).

⁷L. Fister, X. M. Li, T. Novet, J. McConnell, D. C. Johnson, *J. Vac. Sci. Technol. A* **11**, 3014 (1993).

⁸L. J. van der Pauw, *Philips Res. Rep.* **13**, 1 (1958).

⁹In circular shaped samples discontinuous jumps in the sheet resistance were sometimes observed during temperature cycling, occurring simultaneously with discontinuous changes in the distribution of current in the sample. The cross shape effectively eliminated these sudden jumps in the measured resistance and the current distribution.

¹⁰This value of the resistivity is different from the value 230 $\mu\Omega \text{ cm}$ reported by the authors. The discrepancy arises from fitting the data in different forms; we calculate 250 $\mu\Omega \text{ cm}$ from our approximation to their data set when fitting resistance versus inverse molybdenum thickness.

¹¹J. H. Mooji, *Phys. Status Solidi A* **17**, 521 (1973).

¹²C. C. Tsuei, *Phys. Rev. Lett.* **57**, 1943 (1986).

¹³A. B. Kaiser, *Phys. Rev. Lett.* **58**, 1384 (1987).

¹⁴B. L. Altshuler and A. G. Aranov, in *Electron-electron Interactions in Disordered Systems*, edited by A. L. Efros and M. Pollak (North Holland, Oxford, 1985), p. 1.

- ¹⁵Y. Ijdiyaou, M. Azizan, E. L. Ameziane, M. Brunel, and T. A. Nguyen Tan, *Appl. Surf. Sci.* **55**, 165 (1992).
- ¹⁶T. A. Nguyen Tan, M. Azizan, and R. C. Cinti, *Surf. Sci.* **162**, 651 (1985).
- ¹⁷K. Holloway, B. D. Khiem, and R. Sinclair, *J. Appl. Phys.* **65**, 474 (1989).
- ¹⁸R. S. Rosen, D. G. Stears, M. A. Viliardos, M. E. Kassner, S. P. Vernon, and C. Yuanda, *Appl. Opt.* **32**, 6975 (1993).